Experimental investigation of the aeroelastic behavior of a complex prismatic element

Cung Huy Nguyen, Andrea Freda, Giovanni Solari and Federica Tubino[*]

*Department of Civil, Chemical and Environmental Engineering (DICCA), University of Genoa,
Via Montallegro 1, 16145 Genoa, Italy*

Abstract.   Lighting poles and antenna masts are typically high, slender and light structures. Moreover, they are often characterized by distributed eccentricities that make very complex their shape. Experience teaches that this structural type frequently suffers severe damage and even collapses due to wind actions. To understand and interpret the aerodynamic and aeroelastic behavior of lighting poles and antenna masts, this paper presents the results of static and aeroelastic wind tunnel tests carried out on a complex prismatic element representing a segment of the shaft of such structures. Static tests are aimed at determining the aerodynamic coefficients and the Strouhal number of the test element cross-section; the former are used to evaluate the critical conditions for galloping occurrence based on quasi-steady theory; the latter provides the critical conditions for vortex-induced vibrations. Aeroelastic tests are aimed at reproducing the real behavior of the test element and at verifying the validity and reliability of quasi-steady theory. The galloping hysteresis phenomenon is identified through aeroelastic experiments conducted on increasing and decreasing the mean wind velocity.

1. Introduction

Lighting poles and antenna masts are structures typically endowed with relevant height, slenderness and lightness. Moreover, they are often characterized by distributed eccentricities due to features like stairs, cable bundles and solar panels, applied to the shaft, as well as lighting devices, balcony, antennas and parabolas, put at the top, which make very complex their shape.

In order to interpret the wind-induced damage and collapses frequently suffered by this structural type, the authors of the present paper have recently investigated the aeroelastic stability and the wind-excited behavior of lighting poles and antennas masts (Nguyen *et al.* 2015), making recourse to quasi-steady theory based on wind tunnel tests carried out on static sectional models. This research pointed out that structures with specific configurations may face with strong dynamic responses and a wide set of unstable phenomena that can be mainly traced to the galloping family. Such phenomena occur as single-degree-of-freedom (SDOF) crosswind

---

∗Corresponding author, Ph.D., E-mail: federica.tubino@unige.it

oscillations related to the first or upper crosswind modes, or as complex oscillations coupling the alongwind and crosswind motion likewise different modes of vibration.

In wind engineering, galloping occurrence is commonly investigated as a SDOF crosswind oscillation through the well-known Glauert-Den Hartog's method (Glauert 1919, Den Hartog 1932); this method is based on quasi-steady theory and on a linear expansion of the aerodynamic force. Retaining non-linear terms in such expansion, a number of models has been formulated to evaluate galloping oscillation amplitude; among many others, the first and most famous models were developed by Parkinson and Brooks (1961) and by Parkinson and Smith (1964).

According to quasi-steady theory, the theoretical prediction of galloping occurrence is based on the aerodynamic coefficients that are usually derived from static wind tunnel tests on sectional models. Within the framework of a wide review of the galloping phenomenon, Païdoussis *et al.* (2010) provided such data for models with simple cross-sections, namely rectangular, D and L-shape, circular, triangular and elliptical elements.

Aeroelastic wind tunnel tests on prismatic elements with various cross-section shapes are usually conducted in order to verify the theoretical prediction of the critical velocity and the vibration amplitude during galloping occurrence. Worth noting experiments were carried out by Parkinson and Smith (1964) and by Novak (1969) on square sections, by Slater (1969) on L-shape sections. More recently, static and/or dynamic parametric studies have been carried out on triangular shapes (Alonso and Meseguer 2006, Alonso *et al.* 2012), on biconvex cross-sections (Alonso *et al.* 2009), on trapezoidal sections (Kluger *et al.* 2013) and on rhombic sections (Alonso *et al.* 2009, Ibarra *et al.* 2014). Those studies showed a substantial agreement between the experimental results and the theoretical predictions provided by the formulations presented by Parkinson and Smith (1964) and by Novak (1969). They also pointed out the existence of the galloping hysteresis phenomenon, namely the occurrence of different galloping oscillation amplitudes at the same wind velocity, depending on whether the wind velocity is increased or decreased.

To verify the precision and reliability of quasi-steady theory in predicting the aeroelastic instability of complex lighting poles and antenna masts, the present paper illustrates the results of static and aeroelastic wind tunnel tests conducted on a rigid sectional model representative of a typical segment of this structural type. The used values of mass, characteristic length and damping provide Scruton numbers typical of real wind-sensitive structures. Analogous studies have been recently performed by Li *et al.* (2014) to investigate the influence of the presence of lamps on the aerodynamic stability of stay cables, showing the galloping potential of a cable-lamp model.

In the present paper, static tests have been carried out with the aim of providing aerodynamic coefficients and the Strouhal number of a reference sectional model on varying the Reynolds number. Aerodynamic coefficients are used to determine the critical galloping velocity through quasi-steady theory. The Strouhal number is used to determine the critical velocity due to vortex shedding, also in order to check the potential interactions between vortex shedding and galloping. Aeroelastic tests have been conducted to investigate the real behavior of the sectional model, including the critical instability conditions and the post-critical oscillation amplitude. During such tests, the hysteresis phenomenon has been deeply investigated for different values of some key parameters. Finally, the results achieved by static and aeroelastic tests are compared and critically discussed.

2. Quasi-steady approach to galloping analysis

Let us consider a prismatic rigid element immersed in a flow field with mean velocity U, vibrating in the crosswind direction y with velocity $\dot{y}$. The equation of motion is given by

$$\ddot{y} + 2\omega\xi\dot{y} + \omega^2 y = \frac{1}{m}F_y \tag{1}$$

where ω, ξ, m, and F_y are the element circular frequency, damping coefficient, mass per unit length, and aerodynamic force per unit length, respectively.

Adopting quasi-steady hypothesis (Blevins 1990), the aerodynamic force F_y is expressed as

$$F_y = \frac{1}{2}\rho U^2 b C_L - \frac{1}{2}\rho U b \left(C_D + C_L'\right)\dot{y} \tag{2}$$

ρ, b, C_D and C_L' being the air density, the characteristic width of the cross-section, the drag coefficient and the prime derivative of the lift coefficient with respect to the angle of attack, respectively.

In order to carry out stability analysis, Eq. (2) is replaced into Eq. (1) neglecting the static term. Thus, the equation of motion can be rewritten as

$$\ddot{y} + 2\omega\left(\xi + \xi_a\right)\dot{y} + \omega^2 y = 0 \tag{3}$$

where ξ_a is the aerodynamic damping coefficient, defined as

$$\xi_a = \frac{\rho b U \left(C_D + C_L'\right)}{4m\omega} \tag{4}$$

The necessary condition of instability is then given by (Glauert 1919, Den Hartog 1932)

$$C_D + C_L' < 0 \tag{5}$$

The element is unstable if the total damping ($\xi + \xi_a$) in Eq. (3) is less than or equal to zero. Zeroing such total damping, the critical velocity results

$$U_{cr,DH} = -\frac{4\omega\xi m}{\rho b (C_D + C_L')} = -\frac{\omega b}{\pi(C_D + C_L')}Sc \tag{6}$$

where Sc is the Scruton number

$$Sc = \frac{4\pi m\xi}{\rho b^2} \tag{7}$$

Relationships aimed at generalizing Eq. (6) to real vertical structures are given by Nguyen *et al.* (2015).

Expanding the aerodynamic force F_y in Taylor series and taking the nonlinear terms into account, Parkinson and Smith (1964) solved Eq. (1) and evaluated the post-critical oscillation amplitude. In that study, the analysis of a square section cylinder showed the occurrence of the galloping hysteresis phenomenon. Extending the investigations of Parkinson and Smith, Novak (1969) obtained the analytical solution of the oscillation amplitude in the hysteresis zone. Besides,

he pointed out the existence of a so-called "universal curve" on which, at a given angle of attack, the oscillation amplitudes related to different values of the structural damping fall down; this curve was provided in a coordinate system ($\lambda_N U_r$, $\lambda_N y_r$), where

$$\lambda_N = \frac{n}{2\xi} \ ; \ U_r = \frac{U}{\omega b}; \ y_r = \frac{y}{b} \ ; \ n = \frac{\rho b^2}{2m} \tag{8}$$

In Eq. (8), the non-dimensional quantities λ_N, U_r, y_r, and n are referred to as the Novak's coefficient, the reduced velocity, the reduced oscillation amplitude, and the mass parameter, respectively.

Based on Eq. (6), the critical galloping value of the reduced wind velocity according to Den Hartog criterion is given by

$$U_{r,cr,DH} = -\frac{Sc}{\pi(C_D + C'_L)} \tag{9}$$

In accordance with Novak's study, the universal curve is independent of element parameters such as the natural frequency, mass, stiffness and damping. Moreover, the Novak's universal curve does not depend on the static aerodynamic coefficients and can be built without carrying out static wind tunnel experiments. The results of the aeroelastic wind tunnel tests carried out on L-sections by Slater (1969) and on rectangular sections by Novak (1969, 1972) matched with the theoretical "universal curve". Using a different analytical approach, Kluger *et al*. (2013) confirmed such an agreement. It is worth noting that in those studies the aerodynamic coefficients were unaffected by the Reynolds number. However, if they depended on the Reynolds number, and thus on the mean wind velocity, the hysteresis regime might be modified; this might lead to some doubts on the classical existence of the "universal curve".

3. Wind tunnel tests

Static and aeroelastic experiments on the sectional model of a typical segment of the shaft of a complex antenna mast have been conducted in the wind tunnel laboratory at the Department of Civil, Chemical and Environmental Engineering (DICCA) of the University of Genoa. The wind tunnel is a closed loop subsonic circuit, with a cross section 1700 mm wide and 1350 mm high. Static tests are aimed to derive the static aerodynamic coefficients and the Strouhal number as functions of the angle of attack. Aeroelastic tests are aimed to determine structural motion amplitude for different values of the wind velocity.

Fig. 1 sketches the cross-section of the model, pointing out the presence of eccentric stairs and cable bundles. The model has a geometric scale 1:5 and has been used for both static and aeroelastic tests. The angle of attack α is defined as shown in the figure. The model is realized through the assemblage of aluminum profiles, and has a span length $l = 500$ mm. The cable system is modeled by a rectangular cylinder with sides 60 mm x 30 mm. The ladder is modeled by a series of steel bars with length 80 mm.

The element model has been mounted in cross-flow configuration on a force balance realized by six resistive load cells. End plates have been installed at the extremities of the model to maintain two-dimensional flow conditions and to separate the model from the boundary layer of

the wind-tunnel lateral walls. Fig. 2 shows the wind tunnel setups for the static (Fig. 2(a)) and aeroelastic (Fig. 2(b)) sectional model tests, respectively.

The force balance measurements have been used to evaluate the steady aerodynamic drag and lift coefficients and the Strouhal number defined as

$$C_D = \frac{\mathrm{E}[F_D]}{0.5\rho b l U^2} \; ; \; C_L = \frac{\mathrm{E}[F_L]}{0.5\rho b l U^2} \; ; \; St = \frac{f_s b}{U} \tag{10}$$

where E[•] is the statistic average operator, implemented as a time average adopting the hypothesis of ergodic behavior; b=80 mm is the characteristic width of model cross-section; F_D and F_L are, respectively, the measured drag and lift forces; U is the undisturbed mean wind velocity; f_s is the vortex shedding frequency estimated by fitting the power spectral density of F_L in the neighborhood of its peak through a Gaussian function. Based on St, the reduced critical velocity associated with the vortex shedding is given by

$$U_{r,cr,s} = \frac{1}{2\pi St} \tag{11}$$

No data correction has been adopted with reference to the blockage ratio, since it is very low (<2.5%). The influence of the Reynolds number referred to the diameter of the circular cylinder (Re = Ub/ν, ν=1.5·10^{-5} m^2/s) has been investigated by varying the mean wind velocity in the range $U \cong 5 - 25$ m/s (Re = 2.67·10^4÷1.33·10^5).

During aeroelastic tests, the model has been mounted on a system of springs. Undesired modes of vibration as the rocking motion have been avoided. For each experimental setup, the structural damping and the natural frequency of the model have been evaluated during the test. They have been derived from the time history of the decaying vibration, after disturbing the model from the equilibrium position in absence of wind flow. The element displacement has been recorded through a system of four laser distance sensors.
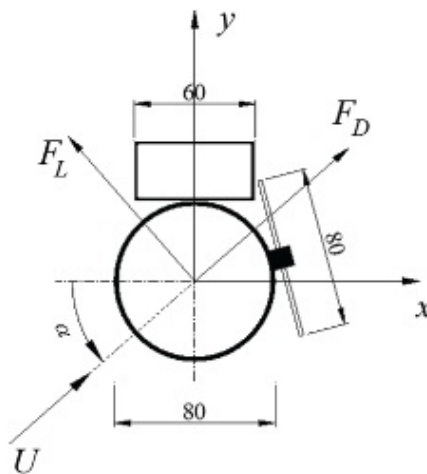

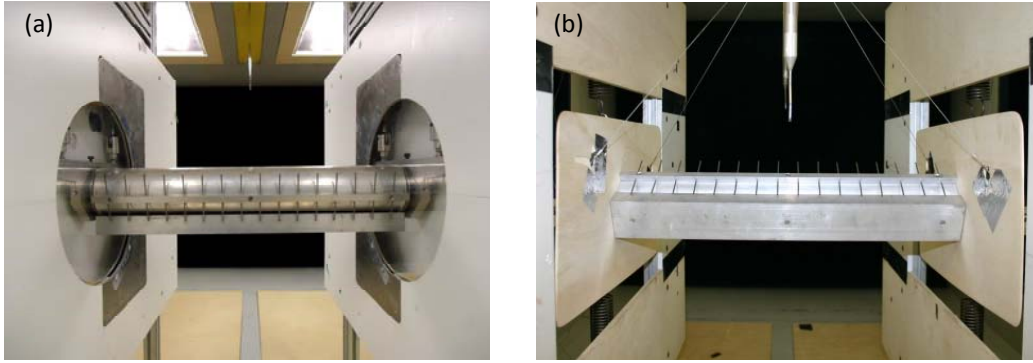Fig. 1 Shaft with eccentric appendages: cross section of the model (units: mm)

Fig. 2 Wind tunnel test setup: (a) static test and (b) aeroelastic test

4. Static test results

Static tests have been conducted firstly for angles of attack α varying from 0° to 350° with step 10° for Re = $2.8 \cdot 10^4$, $5.6 \cdot 10^4$ and $8.6 \cdot 10^4$. Due to the complexity of the cross section shape, such tests have been regarded as a preliminary appraisal of the general aerodynamic behavior of the sectional element. So, starting from the results of these tests, new static tests have been conducted in order to investigate two specific domains of the angle of attack with step 1°. They correspond to the conditions providing, respectively, the maximum and minimum values of $(C_D + C'_L)$. Such a campaign has been carried out for Re = $2.8 \cdot 10^4$, $5.6 \cdot 10^4$, $8.6 \cdot 10^4$ and $1.2 \cdot 10^5$. Figs. 3-7 plot, respectively, the drag coefficient C_D, the lift coefficient C_L, the coefficient $(C_D + C'_L)$, the Strouhal number St, and the reduced critical velocity associated with the vortex shedding $U_{r,cr,s}$, for the Reynolds numbers Re = $5.6 \cdot 10^4$, Re = $8.6 \cdot 10^4$, and, when available, Re = $1.2 \cdot 10^5$. In each figure, the left panel (a) provides the results of the tests carried out on varying α from 0° to 350° with step 10°; the right panels (b) and (c) provide the results of the tests carried out in the ranges α = 67° - 74° and α = 265° - 275°, with step 1°, corresponding to the maximum and minimum values of $(C_D + C'_L)$, respectively. It is worth noting that, especially in the domain in which $(C_D + C'_L)$ assumes negative values, all the measured quantities are extremely sensitive even to small changes of the angle of attack. It is also noticeable that, if the element was composed only by the cylinder and by the rectangle, the static aerodynamic coefficients and the Strouhal number would be symmetric with respect to the direction 180°. The presence of the stair, even if quite small compared with the size of the other elements, causes a relevant asymmetry of the aerodynamic coefficients.

The prime derivative of the lift coefficient with respect to the angle of attack C'_L has been obtained through a smoothing spline approximation. The spline parameters have been chosen in order to provide the best fitting. The shadowed areas in Fig. 5(a) correspond to the domains in which $(C_D + C'_L)$ is negative, i.e., the structure may be unstable according to the Glauert-Den Hartog's criterion given in Eq. (5). It is worth noting that $(C_D + C'_L)$ strictly depends on how the aerodynamic coefficients are fitted. A little change of the fitting curve can noticeably modify the $(C_D + C'_L)$ values. Furthermore, Fig. 5(c) shows that the domain in which $(C_D + C'_L)$ is negative is

very sharp and (C_D+C'_L) drastically changes for tiny changes of α; for instance, at Re = $1.2 \cdot 10^5$, (C_D+C'_L) varies between -8.8 and -33.7 on varying α between 270° and 271.5° (Fig. 5(c)). A different value was found based on preliminary tests carried out in steps of 10°. This means that the Glauert-Den Hartog critical velocity is very sensitive to small variations of α. It is also worth noting that the measurements of the angle of attack have been performed by a digital protractor whose instrumental error is ±0.2°; so, static test results may be slightly biased.
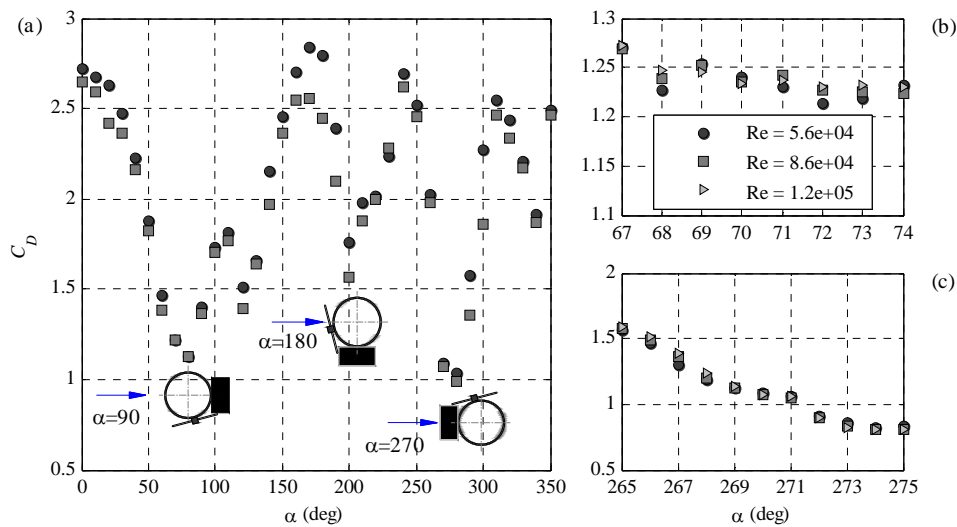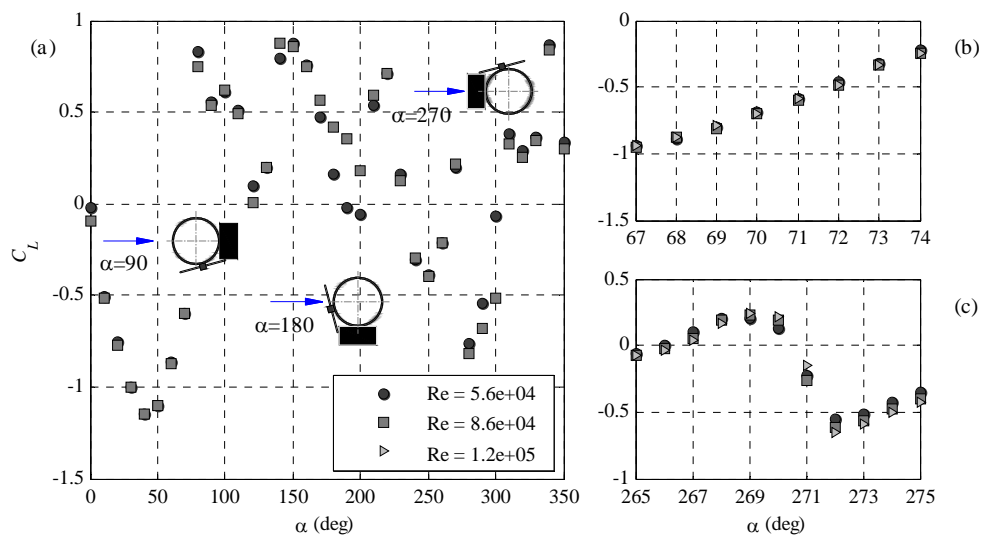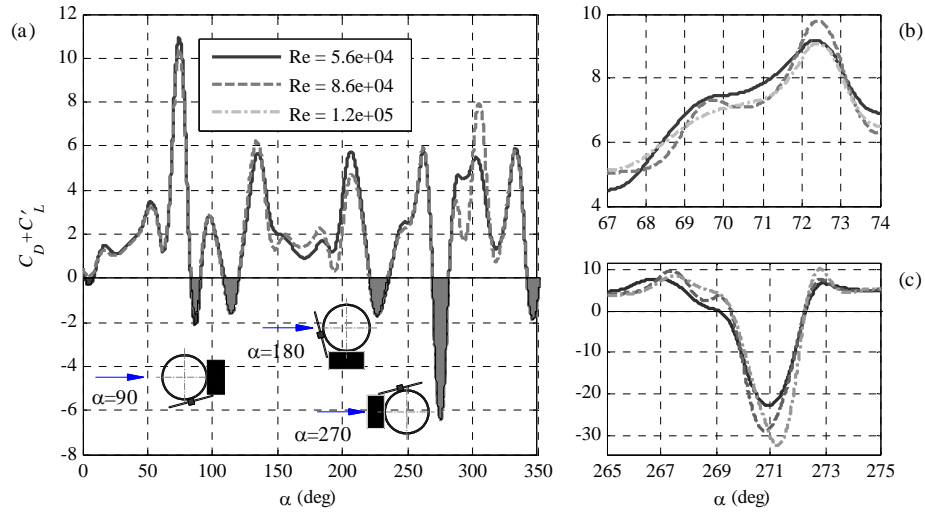

Fig. 3 Drag coefficient
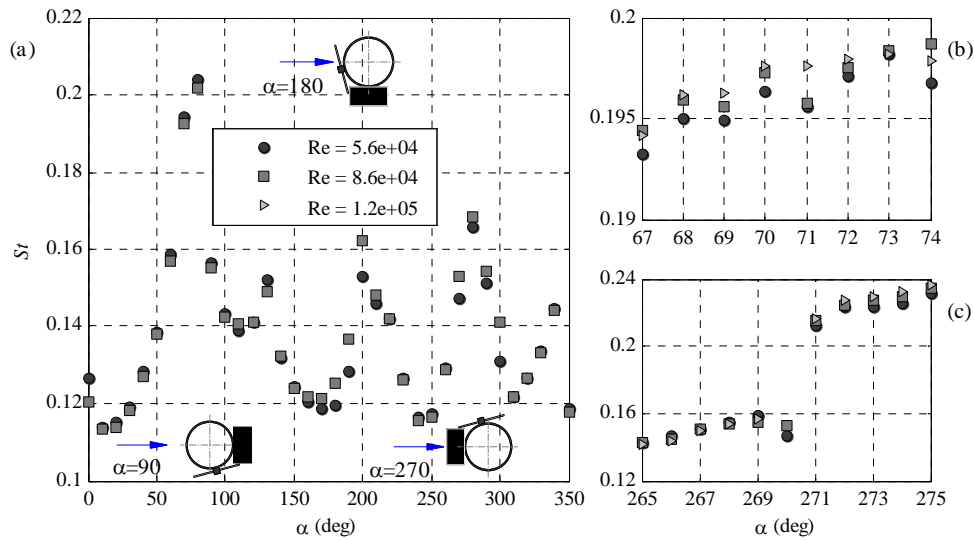

Fig. 4 Lift coefficient

Fig. 5 Coefficient $(C_D + C'_L)$

Fig. 6 Strouhal number

Fig. 6 shows that the Strouhal number *St* significantly changes in the range $\alpha = 265° - 275°$, assuming values between 0.11 and 0.21. Looking more in detail the range $\alpha = 269° - 271°$, there is a remarkable change of *St* close to $\alpha = 270°$, where $(C_D + C'_L)$ assumes large negative values leading to potential galloping instability. The reason may due to the fact that, at this angle of attack,

the mean wind direction is orthogonal to the rectangular profile that idealizes the cable bundles; this may give rise to a critical direction strongly affecting the stability condition of the model. It is also worth noting that the relevant variability of the shedding frequency implies that the structure may be particularly susceptible to Vortex-Induced-Vibrations (VIV) in a wide range of wind velocities. An analogous remark was pointed out by Fleck (2001), who conducted wind tunnel tests on a combined circular-rectangular prism with similar aspect ratio.

Concerning the influence of the Reynolds number on the aerodynamic coefficients, Figs. 3 and 4 and Figs. 6 and 7 show that this parameter slightly affects the drag and lift coefficients, the Strouhal number, and the reduced critical velocity associated with the vortex shedding; it is worth noting, however, that no regular vortex shedding has been observed for $Re = 1.2 \cdot 10^5$. On the contrary, Fig. 5 shows that the Reynolds number strongly influences $(C_D + C'_L)$, particularly in the range $\alpha = 269°$ -272°, where $(C_D + C'_L)$ is negative (Fig. 5(c)); for example, at $\alpha = 271.5°$, $(C_D + C'_L)$ = -26.7 for $Re = 8.6 \cdot 10^4$, while $(C_D + C'_L) = -20.7$ for $Re = 1.2 \cdot 10^5$. Such a large difference has a deep impact on evaluating the critical galloping velocity through Eq. (6); this remark casts doubts on the reliability of quasi-steady theory in the present context.

5. Aeroelastic test results

To analyze the aeroelastic behavior of the sectional element and to verify the reliability of quasi-steady theory in predicting the critical conditions for galloping occurrence, aeroelastic tests have been carried out at three angles of attack: $\alpha = 70°$, where $(C_D + C'_L)$ is positive (Fig. 5(b)), $\alpha = 270°$ and $\alpha = 271°$, where $(C_D + C'_L)$ is negative (Fig. 5(c)). For each α value, tests have been conducted increasing and decreasing the wind velocity with a fine discretization, aiming at capturing the occurrence of the hysteresis phenomenon. Moreover, at $\alpha = 270°$ and $\alpha = 271°$, where the structural element is prone to gallop, tests have been carried out for different values of the structural damping in order to investigate the influence of this parameter on the aeroelastic behavior. In every case the crosswind oscillation amplitude has been measured in correspondence of stable limit oscillation cycles.

Table 1 shows the values of the model mass per unit length m, of the structural damping coefficient ξ, and of the natural frequencies $f = \omega/2\pi$ corresponding to different setups. In spite of the very low values of ξ, the Scruton number Sc (Eq. (7)) assumes values in the range from 3 to 15.5, typical of real wind-sensitive structures.

Table 1 Structural model parameters

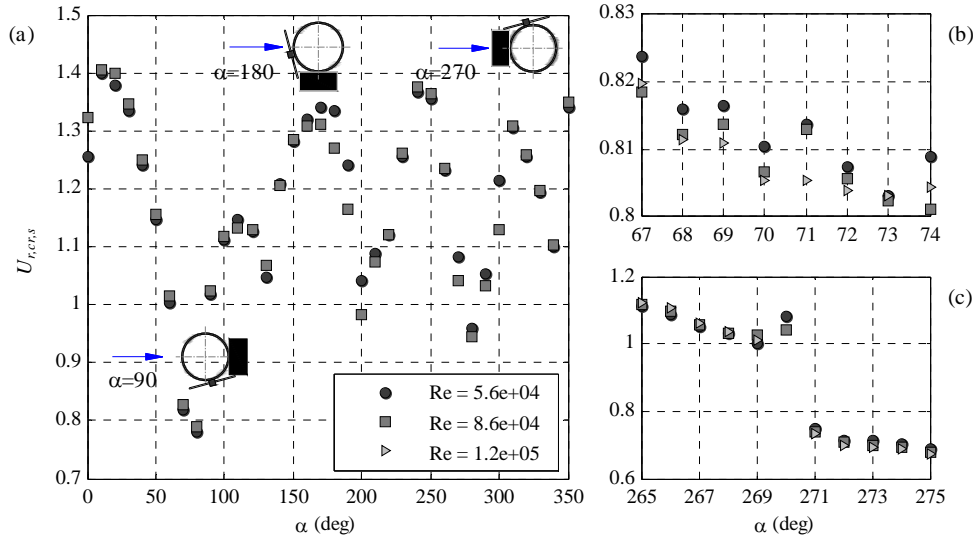| m (kg/m)	ξ (%)			f (Hz)		
	$\alpha=70°$	$\alpha=270°$	$\alpha=271°$	$\alpha=70°$	$\alpha=270°$	$\alpha=271°$
		0.024	0.027		5.42	5.43
7.88	0.13	0.045	0.041	5.49	5.28	5.32
		0.125	0.046		5.50	5.31

Fig. 7 Reduced critical velocity due to vortex shedding

Fig. 8 plots the reduced oscillation amplitude y_r versus the reduced velocity U_r (Eq. (8)) at $\alpha =$ 70°, 270° and 271°, for the different setups described in Table 1. The results associated with $\alpha =$ 270° and $\alpha = 271°$ include tests for different values of ξ. It is apparent that the oscillation amplitude at $\alpha = 70°$ is considerably smaller than that at $\alpha = 270°$ and $\alpha = 271°$; besides, it tends to slightly increase on increasing the mean wind velocity. This trend occurs because, at $\alpha = 70°$, $(C_D+C'_L)$ is positive. It follows that no instability occurs and the oscillation is due to buffeting. It is worth mentioning that, in this case, no measurement has been carried out for reduced velocities $U_r < 2$. On the other hand, at $\alpha = 270°$ and $\alpha = 271°$, large oscillation amplitudes occur around $U_r = 0.7$ and for $U_r > 2.2$. Making reference to Fig. 7(c), it is apparent that the oscillations for $U_r = 0.7$ are related to VIV. On the contrary, the oscillations for $U_r > 2.2$ are caused by galloping. As a consequence, the aeroelastic tests confirm the validity of using quasi-steady theory to predict the critical wind direction that gives rise to galloping. In other words, quasi-steady theory is successful in providing the necessary condition for galloping occurrence (Eq. (5)).

A worth noting remark provided by Fig. 8 is that hysteresis galloping has been detected at both $\alpha = 270°$ and $\alpha = 271°$. Fig. 9 provides a deeper insight into this phenomenon, considering also the role of structural damping. Fig. 9(a) shows the reduced oscillation amplitude y_r for $\alpha = 270°$ and for $\xi = 0.024\%$, 0.045% and 0.125%. Fig. 9(b) shows the reduced oscillation amplitude y_r for $\alpha = 271°$ and for $\xi = 0.027\%$, 0.041% and 0.046%. Hysteresis cycles are indicated by continuous lines.

It can be witnessed that, at the lowest structural damping ($\xi = 0.024\%$ for $\alpha = 270°$ and $\xi = 0.027\%$ for $\alpha = 271°$), the oscillation amplitude increases linearly on increasing the reduced velocity. At higher structural damping ($\xi = 0.045\%$ and 0.125% for $\alpha = 270°$, and $\xi = 0.041\%$ and 0.046% for $\alpha = 271°$), instead, such linearity disappears and galloping hysteresis occurs. The critical velocity at which the element vibrates with very large amplitude depends on whether the

tested-velocity increases or decreases. In addition, the hysteresis regime is larger for higher structural damping.

The above observations stress the influence of the structural damping not only on oscillation amplitude but also on hysteresis occurrence. At a given angle of attack, i.e., for a certain aerodynamic coefficient ($C_D + C'_L$), as derived from static wind tunnel tests, the aeroelastic behavior is completely different for different structural damping values. This contradicts the results provided by Luo *et al.* (2003) and by Barrero-Gil *et al.* (2009), who claimed that galloping hysteresis occurrence depends on the inflection points of the curve $C_D + C'_L$, and by Kluger *et al.* (2013), who stated that only the static aerodynamic coefficients affect hysteresis existence.

One may argue that small values of the structural damping may reduce the critical galloping velocity, giving rise to an interaction between galloping and VIV; however, even considering the cases $\xi = 0.024\%$ ($\alpha = 270°$) and $\xi = 0.027\%$ ($\alpha = 271°$), the ratio between the reduced critical galloping velocity $U_{r,cr,a}$ and the reduced critical vortex shedding velocity $U_{r,cr,s}$ ($U_{r,cr,a}/U_{r,cr,s}$) is respectively about 2.4 and 3.6, therefore relatively larger than the value 2 suggested by Blevins (1977) in order to exclude galloping and VIV interaction. Also, $2\pi U_r$ is about 15.7 for $\xi = 0.024\%$ ($\alpha = 270°$) and 17 for $\xi = 0.027\%$ ($\alpha = 271°$). The literature is usual to assume that galloping occurrence is not disrupted by VIV provided that $2\pi U_r > 10$, as proposed by Fung (1955) and Blevins (1977), 20, by Blevins (1990), or 30, by Bearman *et al.* (1987). Nevertheless, no interaction between galloping and VIV has been observed during the experiments.
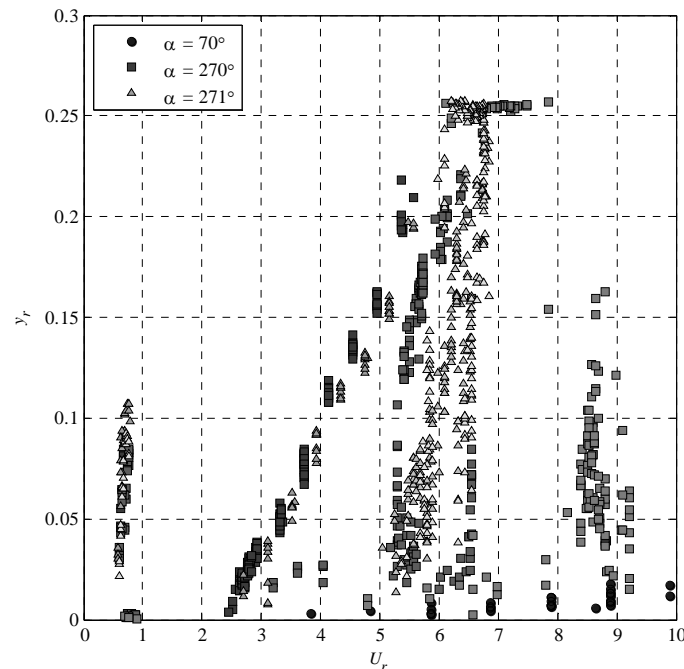

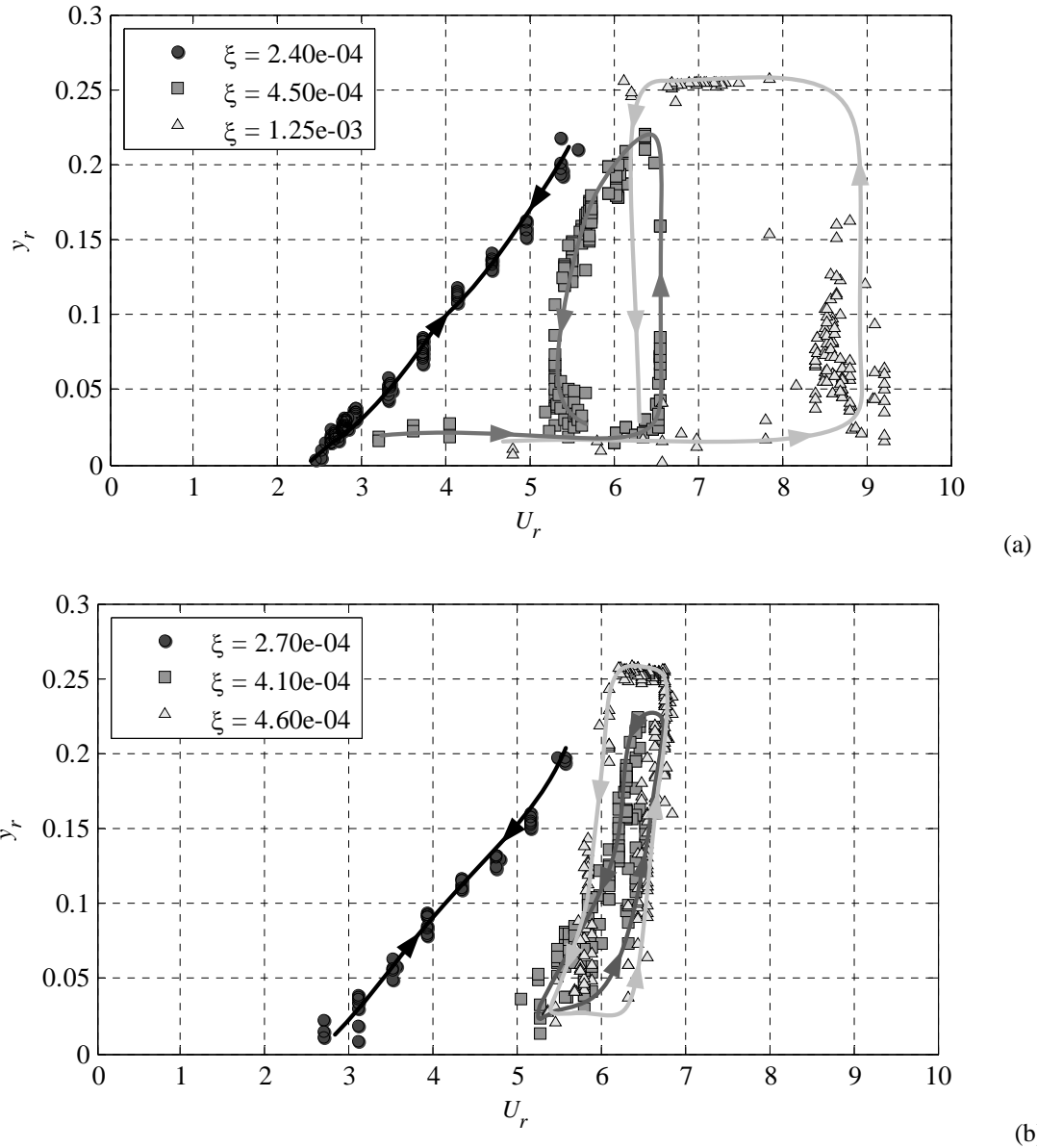Fig. 8 Reduced amplitude versus reduced velocity at the angles of attack 70°, 270° and 271°

Fig. 9 Reduced amplitude versus reduced velocity at the angles of attack 270°(a) and 271°(b)

Fig. 10 shows the results plotted in Fig. 9 in the scaled axes ($\lambda_N U_r$, $\lambda_N y_r$), where λ_N is given by Eq. (8). It is worth noting that the results do not collapse on a "universal curve", as stated by Novak (1969). At $\alpha = 270°$ (Fig. 10(a)), the responses associated with different values of ξ are clearly separated. At $\alpha = 271°$ (Fig. 10(b)), the aeroelastic behavior related to different values of ξ are more similar but the distinction remains visible. It should be emphasized that Novak's

experiments were conducted at structural damping values much higher than those in this paper. Additionally, the values of ξ adopted by Novak were not so far from each other. In the present paper, smaller values of ξ in a wider range are considered to reproduce the typical Scruton numbers of wind-sensitive structures and of elements prone to instability. It seems reasonable to argue that in these conditions the hysteresis regions are modified in such a way as to avoid the collapse of oscillation amplitudes onto a universal curve.
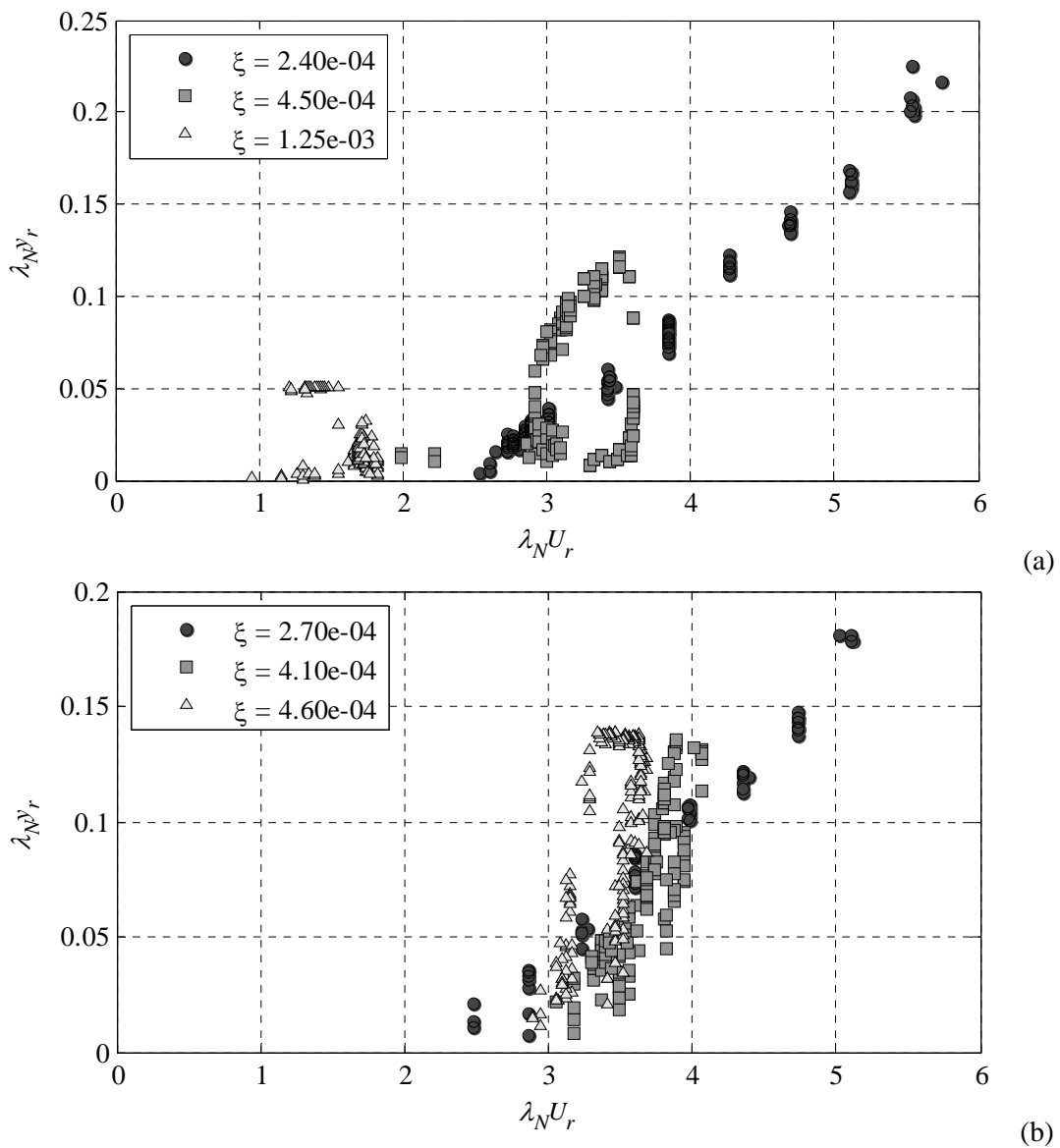

Fig. 10 Novak's reduced amplitude versus reduced velocity at α=270°(a) and α=271°(b)

Comparing the responses for $\alpha = 270°$ and $\xi = 0.045\%$ (Figs. 9(a) and 10(a)) and for $\alpha = 271°$ and $\xi = 0.041\%$ (Figs. 9(b) and 10(b)), it is apparent that a small change of the angle of attack (only 1°) provides significant changes of the aeroelastic behavior. The oscillations at $\alpha = 270°$ start increasing at a $\lambda_N U_r$ value lower than the one at $\alpha = 271°$. In addition, the hysteresis regime at $\alpha = 270°$ is larger than the one at $\alpha = 271°$. This observation points out that the aeroelastic response is very sensitive to the sectional configuration and to the structural damping.

6. Comparison between static and aeroelastic test results

Due to its simplicity, Glauert-Den Hartog's theory has been widely applied to determine the critical conditions for galloping occurrence. This section provides a verification of this theory, for the case study considered, based on the results obtained from static and aeroelastic tests.

First of all, as already noted in Section 5, the results shown in Fig. 8 confirm the validity of Eq. (5) to predict the critical wind directions that give rise to galloping occurrence.

To verify the reliability of Eq. (6) in estimating the critical galloping velocity, the reduced critical velocities obtained from static and aeroelastic tests at $\alpha = 270°$ and $\alpha = 271°$ are compared. As mentioned in Section 4, $(C_D + C'_L)$ is strongly dependent on the angle of attack α and on the Reynolds number Re. Thus, the reduced critical velocity provided by Glauert-Den Hartog's criterion, Eq. (9), is strongly dependent on α and Re. Consequently, aiming at comparing the results related to $\alpha = 270°$, $U_{r,cr,DH}$ is determined with reference to the $(C_D + C'_L)$ values in the range $\alpha = 269.5° - 270.5°$, i.e., $\pm 0.5°$ around $\alpha = 270°$, for different Reynolds numbers. Analogously, aiming at comparing the results related to $\alpha = 271°$, $U_{r,cr,DH}$ is determined with reference to the $(C_D + C'_L)$ values in the range $\alpha = 270.5° - 271.5°$, for different Reynolds numbers.

Table 2 reports the $(C_D + C'_L)$ values in the range $\alpha = 269.5° - 271.5°$, for different Reynolds numbers. The last two columns are built in such a way that, for $\alpha = 270°$, $(C_D + C'_L)|_{min}$ and $(C_D + C'_L)|_{max}$ are respectively the minimum and maximum values of $(C_D + C'_L)$ in the range $\alpha = 269.5° - 270.5°$. The case in which $\alpha = 271°$ is analogous. In correspondence of each value of $(C_D + C'_L)|_{min}$ and $(C_D + C'_L)|_{max}$, the values of $U_{r,cr,DH}|_{min}$ and $U_{r,cr,DH}|_{max}$ are determined for different values of the structural damping.

Table 3 compares the values of $U_{r,cr,DH}|_{min}$ and $U_{r,cr,DH}|_{max}$ with the critical value of wind velocity obtained from aeroelastic tests, $U_{r,cr,a}$. It shows that, for $\alpha = 270°$, $U_{r,cr}$ is in the range of $U_{r,cr,DH}$ between $U_{r,cr,DH}|_{min}$ and $U_{r,cr,DH}|_{max}$. Thus, in this case, it is trustworthy to estimate the critical velocity based on quasi-steady theory. However, for $\alpha = 271°$, $U_{r,cr,a}$ is much higher than $U_{r,cr,DH}|_{max}$, i.e., $U_{r,cr,a}$ is completely outside the range of $U_{r,cr,DH}$ between $U_{r,cr,DH}|_{min}$ and $U_{r,cr,DH}|_{max}$. It is worth noting that the comparison reported in Table 3 does not take into account the influence of the Reynolds number on the critical wind velocity. Considering the Reynolds number effect, Fig. 11 shows the comparison, for different values of the structural damping, between $U_{r,cr,a}$ at $\alpha = 270°$ and $U_{r,cr,DH}$ at $\alpha = 269.5°$ and $\alpha = 270.5°$ (see Table 2).

It can be observed that, for higher structural damping, the value of $U_{r,cr,a}$ tends to be between $U_{r,cr,DH}|\alpha = 269.5°$ and $U_{r,cr,DH}|\alpha = 270.5°$. In other words, in spite of the complexity of the cross-section shape examined here, Glauert-Den Hartog theory is able to provide reasonable values of the critical velocity in specific ranges of the wind direction and of the structural damping.

Table 2 Values of $C_D + C'_L$ for various angles of attack

α		$C_D + C'_L$			$(C_D+C'_L)|_{min}$	$(C_D+C'_L)|_{max}$
		Re=5.6·10⁴	Re=8.6·10⁴	Re=1.2·10⁵		
	269.5°	4.1	1.2	0.4		
270°	270°	11.7	13.2	8.8	0.4	26.7
	270.5°	20.4	26.7	20.7		
	270.5°	20.4	26.7	20.7		
271°	271°	22.7	28.1	30	18.4	30.3
	271.5°	18.4	20.5	30.3		

Table 3 Comparison between the results obtained from static and aeroelastic tests

α	$\xi\,(\%)$	$U_{r,cr,a}$	$U_{r,cr,DH}$	
			$U_{r,cr,DH}|_{min}$	$U_{r,cr,DH}|_{max}$
	0.024	2.5	0.04	2.42
270°	0.045	3.2	0.07	4.54
	0.125	4.8	0.19	12.62
	0.027	2.7	0.04	0.06
271°	0.041	5.1	0.05	0.09
	0.046	5.3	0.06	0.10

7. Conclusions

In this paper, the aerodynamic and aeroelastic behavior of a prismatic element with complex shape has been studied by means of static and aeroelastic wind tunnel experiments. This study stems from a preceding research on the instability of complex lighting poles and antenna masts (Nguyen *et al.* 2015), carried out by using quasi-steady theory and preliminary measurements of the aerodynamic coefficients of static sectional models. The new research does not pursue the aim of investigating the aeroelastic behavior of a specific real structure, but to clarify the reliability of the joint use of quasi-steady theory and static sectional models of complex-shape elements. The results have provided several critical remarks.

Firstly, the complexity of the element cross-section strongly affects the static aerodynamic coefficients and the Strouhal number, which are very sensitive even to small changes of the angle of attack of the wind. The Reynolds number slightly influences the drag and lift coefficients and the Strouhal number, but considerably affects the coefficient $(C_D+C'_L)$.

Secondly, in spite of the complexity of the cross-section shape, Glauert-Den Hartog's theory is able to predict the critical wind directions that give rise to galloping. However, it fails to predict the critical velocity associated with some angles of attack.

Thirdly, at low structural damping values, the galloping oscillation amplitude is almost proportional to the wind velocity. At higher structural damping values, the galloping hysteresis is detected. Analyses also show that both vibration amplitude and hysteresis existence strictly depend on the structural damping. In addition, at least for the examined element, Novak's "universal curve" does not exist.

Finally, several problems of engineering nature arise. Using quasi-steady theory based on static tests on sectional models, Nguyen *et al.* (2015) highlighted the existence of configurations that give rise to unstable phenomena. Making recourse to aeroelastic tests on a rigid sectional model, the present analyses confirm the existence of such phenomena, just in the same situations revealed by quasi-steady theory. In the meanwhile, they raise doubts on the possibility of predicting reliable values of the critical galloping velocity through simplified engineering models based on quasi-steady theory and static wind tunnel tests. The problem deserves further studies.
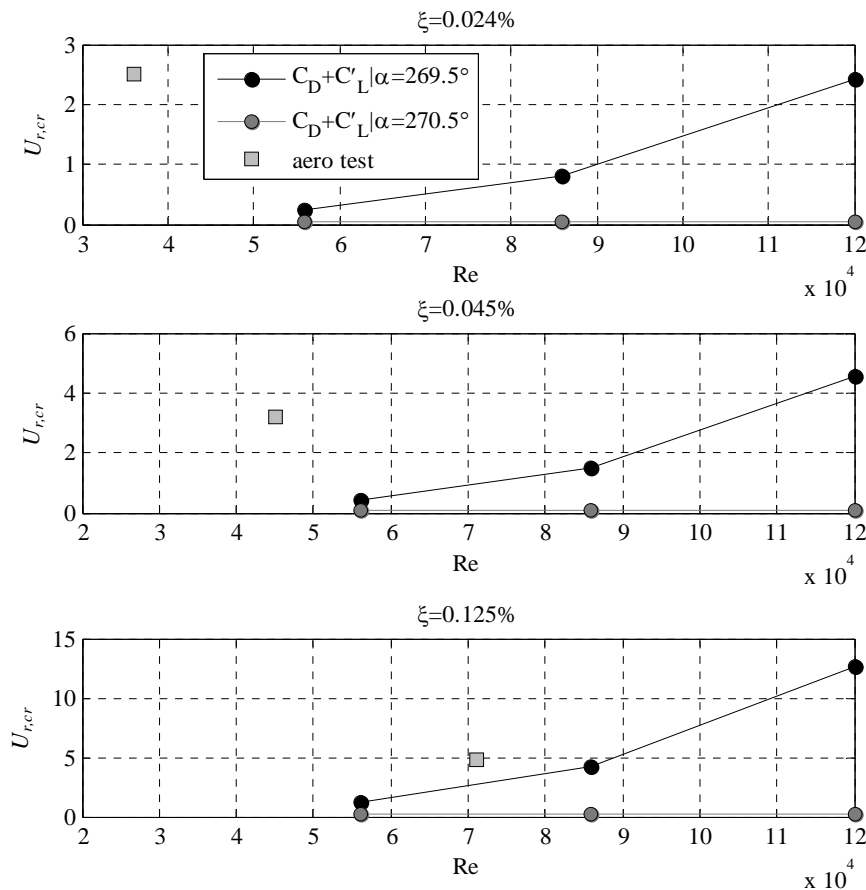

Fig. 11 Comparison of critical velocities obtained from static and aeroelastic tests at $\alpha=270°$

References

Alonso, G. and Meseguer, J. (2006), "A parametric study of the galloping stability of two-dimensional triangular cross-section bodies", *J. Wind. Eng. Ind. Aerod.*, **94**(4), 241-253.

Alonso, G. Valero, E. and Meseguer, J. (2009), "An analysis on the dependence on cross section geometry of galloping stability of two-dimensional bodies having either biconvex or rhomboidal cross sections", *Eur. J. Mech. B. Fluids*, **28**(2), 328-334.

Alonso, G., Sanz-Lobera, A. and Meseguer, J. (2012), "Hysteresis phenomena in transverse galloping of triangular cross-section bodies", *J. Fluid Struct*, **33**, 243-251.

Barrero-Gil, A., Sanz-Andre´s, A. and Alonso, G. (2009), "Hysteresis in transverse galloping: The role of the inflection points", *J. Fluid. Struct.*, **25**(6), 1007-1020.

Bearman, P.W., Gartshore, I.S., Maull, D.J. and Parkinson, G.V. (1987), "Experiments on flow-induced vibration of a square-section cylinder", *J. Fluid Struct.*, **1**(1), 19-34.

Blevins, R.D. (1977), *Flow-Induced Vibration*, Van Nostrand Reinhold, New York, NY, USA.

Blevins, R.D. (1990), *Flow-Induced Vibration*, 2nd Ed., Van Nostrand Reinhold, New York, NY, USA.

Den Hartog, J.P. (1932), "Transmission line vibration due to sleet", *T. Am. Inst. El. Eng.*, **51**, 1074-1076.

Fleck, A. (2001), "Strouhal numbers for flow past a combined circular–rectangular prism", *J. Wind. Eng. Ind. Aerod.*, **89**(9), 751-755.

Fung, Y.C. (1955), *An Introduction to the Theory of Aeroelasticity*, Wiley, New York, NY, USA.

Glauert, H. (1919), "The rotation of an aerofoil about a fixed axis", *(British) Advisory Committee for Aeronautics (ARC) R & M No. 595. Technical Report of ARC for 1918–1919*, 443-447.

Ibarra, D., Sorribes, F., Alonso, G. and Meseguer, J. (2014), "Transverse galloping of two-dimensional bodies having a rhombic cross-section", *J. Sound Vib.*, **333**(13), 2855-2865.

Kluger, J.M., Moon, F.C. and Rand, R.H. (2013), "Shape optimization of a blunt body Vibro-wind galloping oscillator", *J. Fluid. Struct.*, **40**, 185-200.

Li, S.Y., Chen, Z.Q., Dong, G.C. and Luo, J.H. (2014), "Aerodynamic stability of stay cables incorporated with lamps: a case study", *Wind Struct.*, **18**(1), 83-101.

Luo, S.C., Chew, Y.T. and Ng, Y.T. (2003), "Hysteresis phenomenon in the galloping oscillation of a square cylinder", *J. Fluid. Struct.*, **18**(1), 103-118.

Nguyen, C.H., Freda, A., Piccardo, G., Solari, G. and Tubino, F. (2012), "Aeroelastic behavior of complex lighting towers and antenna masts", *Proceedings of the 7th International Colloquium on Bluff Body Aerodynamics and Applications - BBAA VII*, Shanghai, China.

Nguyen, C.H., Freda, A., Solari, G. and Tubino, F. (2015), "Aeroelastic instability and wind-excited response of complex lighting poles and antenna masts", *Eng. Struct.*, **85**, 264-276.

Novak, M. (1969), "Aeroelastic galloping of prismatic bodies", *J. Eng. Mech. Div. - ASCE*, **96**, 115-142.

Novak, M. (1972), "Galloping oscillations of prismatic structures", *J. Eng. Mech. Div.-ASCE*, **98**, 27-46.

Païdoussis, M.P., Price, S.J. and de Langre, E. (2010), *Fluid Structure Interactions Cross Flow Induced Instabilities*, Cambridge University Press, Cambridge, UK.

Parkinson, G.V. and Brooks, N.P.H. (1961), "On the aeroelastic instability of bluff cylinders", *J. Appl. Mech.*, **28**(2), 252-258.

Parkinson, G.V. and Smith, J.D. (1964), "The square prism as an aeroelastic non-linear oscillator", *Q. J .Mech. Appl. Math.*, **17**(2), 225-239.

Slater, J.E. (1969), *Aeroelastic instability of a structural angle section*, Ph.D. Thesis, University of British Columbia, Vancouver, B.C., Canada.

Vio, G.A., Dimitriadis, G. and Cooper, J.E. (2007), "Bifurcation analysis and limit cycle oscillation amplitude prediction methods applied to the aeroelastic galloping problem", *J. Fluid. Struct.*, **23**(7), 983-1011.

CC